Polymer Chemistry

ROYAL SOCIETY OF CHEMISTRY

PAPER

View Article Online
View Journal | View Issue

Cite this: *Polym. Chem.*, 2023, **14**, 1478

Multiphase PCL semi-interpenetrating networks exhibiting the triple- and stress-free two-way shape memory effect†

Koichiro Uto, *[a] Yoshitaka Matsushita [b] and Mitsuhiro Ebara [a]

Multiple- and two-way shape memory polymers (SMPs) are of great interest in the fields of biomedical devices, smart actuators, and soft robotics owing to their ability to achieve complex movements in response to external stimuli. The formation of multiphase polymer networks exhibiting multiple transition temperatures is a versatile design strategy for achieving the multi- or two-way shape memory effect (SME); however, most of them are combinations of heterogeneous polymers, and no system has achieved them using a material composed of only homogeneous polymers. In this study, multiphasic semi-interpenetrating polymer networks (IPNs) with linear poly(ε-caprolactone) (PCL) chains were designed, which are interpenetrated into the crosslinked PCL network and not involved in crosslinking. Furthermore, the effects of the molecular weight and content of linear PCL chains in the semi-IPNs on crystallisation and melting were investigated. While crosslinked PCL exhibits a monophasic and sharp phase transition, the presence of linear PCLs influences the crystallisation/melting behaviour of other chains and determines the broadening of transition and appearance of an additional transition. Thermal, crystal structure, and thermomechanical characterisation revealed that PCL semi-IPNs composed of linear PCLs with a high molecular weight (M_n = 80k) and content (>23 wt%) form distinctly separated crystalline phases and undergoes two-phase melting and crystallisation. As expected, these multiphase PCL semi-IPNs can exhibit triple- and two-way SMEs, opening new avenues for the synthesis and design strategies for multiphase polymer networks of semi-IPNs composed of homologous polymers.

Received 29th December 2022,
Accepted 27th February 2023

DOI: 10.1039/d2py01607a

rsc.li/polymers

Introduction

Shape memory polymers (SMPs) are promising smart materials because they can induce programmed shape changes and motion in response to external stimuli, such as temperature,[1,2] light,[3] electricity,[4] and magnetic fields.[5] The one-way dual shape memory effect (SME), which is a one-way irreversible change from a temporary shape to a permanent shape, is widely known and studied. The programmed motion and shape-changing properties of this type of SMP may be utilised in various fields, including biomedical devices,[6,7] aerospace,[8,9] smart textiles,[10,11] soft robotics,[12,13] and flexible electronics.[14,15] To realise these applications and extend them to more sophisticated ones, it is crucial to develop SMPs that can be programmed to move and change their shape in more complex ways.

Generally, materials exhibiting a one-way dual SME consist of a netpoint (immobilised phase) that allows recovery to a permanent shape because of entropy elasticity, and a switching unit (reversible phase) to fix the deformed shape to a temporary shape.[16,17] The netpoint is formed by physical or chemical crosslinking, and the glass, crystal-amorphous, and liquid crystal phase transitions of polymers are widely used as the switching unit. The semi-crystalline polymer networks, which contain netpoints of chemical crosslinking and employ a crystal-amorphous transition for switching, exhibit T_m-driven sharp responses and high shape memory properties, including chemical stability that can be achieved using simple monophasic polymer network designs. In contrast, the design of multiphase polymer networks can store two or more metastable shapes (temporary shapes), including the most stable shape (permanent shape). Lendlein *et al.* have shown that a copolymer network with two crystalline units can be formed to achieve a triple-SME using a two-step shape programming process.[18,19] Besides this design approach, it is possible to design polymer networks that exhibit the triple-SME by

[a]*Research Center for Functional Materials, National Institute for Materials Science (NIMS), 1-1 Namiki, Tsukuba, Ibaraki 305-0044, Japan.*
E-mail: UTO.Koichiro@nims.go.jp
[b]*Research Network and Facility Services Division, National Institute for Materials Science (NIMS), 1-2-1 Sengen, Tsukuba, Ibaraki 305-0047, Japan*

† Electronic supplementary information (ESI) available. See DOI: https://doi.org/10.1039/d2py01607a

combining various transition temperatures, such as broad transition temperatures[20,21] or, for instance, melting (T_m) and glass transition temperatures (T_g).[22] Because their shape-shifting properties are one-way, triple-SMPs are suitable for applications requiring multiple sequential actuations. Interestingly, the construction of multiphase polymer networks is promising for designing one-way multi-SMPs and two-way SMPs, *i.e.*, reversible systems.[23] Monophasic semi-crystalline polymer networks are known to undergo reversible shape changes owing to crystallisation-induced elongation (CIE) and melting-induced contraction (MIC), which are called quasi-reversible two-way shape changes because they are observed only when the network is stretched by stress loading.[24,25] In a multiphase polymer network with two T_m's, the crystals with the higher T_m behave as a skeleton, *i.e.*, the geometry-determining unit that maintains the orientation of molecular chains by stretching the melted segments toward the lower T_m side, whereas the crystals on the lower temperature side behave as the actuator unit that causes directional crystallisation/melting.[26] Once the network forms the skeleton in a stretched state, it exhibits a fully reversible (two-way) shape change even under stress-free conditions. Because multiphase polymer networks are promising for the fabrication of multi- and 2-way SMPs, forming two distinctly separated phases is crucial. Various multiphase copolymer networks and blend systems have been extensively explored,[27–29] and the miscibility between components, molecular weight, and thermal history are known to affect their thermal properties and crystallisation. To our knowledge, the reported multiphase semi-crystalline polymer networks are combinations of heterogeneous polymers, and the design of multiphase networks comprising homologous polymers has not been investigated.

Poly(ε-caprolactone) (PCL), a semi-crystalline polymer that is biodegradable and approved by the US Food and Drug Administration (FDA), is widely used as a building block to achieve a multi- or two-way SME. We and other groups have reported that radical polymerisation crosslinking of branched PCL macromonomers with polymerizable end groups, such as acrylates, can form chemically stable networks, and the T_m and crystallisation temperature (T_c) of PCL can be precisely tuned by controlling the number of branches and molecular weight.[30–34] The resulting crosslinked PCL is a single-phase polymer network, essentially, a one-way dual SME. For instance, tetra-branched PCLs with a degree of polymerisation of 10 and 100 (4b10 and 4b100PCL) have distinctly different molecular weights. Furthermore, blended crosslinking results in a monophasic polymer network incorporating each polymer despite the macromonomers having different T_m's.[35] Mather *et al.* fabricated PCL semi-IPNs with linear PCL penetrating the PCL network and showed that T_m, T_c, and their enthalpy changes in phase transitions increase with increasing molecular weight (M_w = ~65 000) and content of linear PCL.[36] Furthermore, PCL semi-IPNs exhibited self-healing properties owing to the presence of linear PCLs and demonstrated shape memory assisted self-healing (SMASH) wherein the shape memory of the PCL network can close wounds and

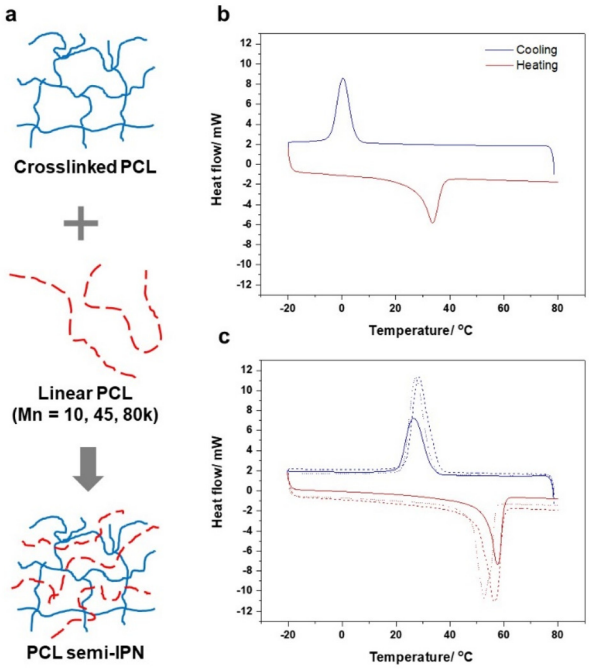

Fig. 1 Design of PCL semi-IPNs. (a) Schematic of PCL semi-IPNs consisting of a crosslinked PCL network and linear PCLs with different molecular weights. DSC curves of (b) the crosslinked 4b10/2b20PCL network and (c) linear PCLs with different molecular weights. Dotted, dashed, and solid lines represent 10k, 45k, and 80k linear PCLs, respectively.

cracks. While these PCL semi-IPNs formed a monophasic blend network, the influence of the PCL network, molecular weight, and the blend content of the linear PCLs on phase formation is ambiguous. In this study, we aimed to fabricate multiphase semi-IPNs composed of homologous polymers, PCLs, to realise triple- and two-way SMEs. Using our previous study on 4b10/2b20 PCL blended crosslinking,[30,31] we fabricated semi-IPNs by adding linear PCLs during the crosslinking reaction (Fig. 1a). The crystallisation of linear PCLs in a PCL network exhibiting relatively low T_m showed strong dependence on the molecular weight and content, and PCL semi-IPNs composed of high molecular weight linear polymers exhibited crystallisation derived from the network and linear polymer. Multiphase PCL semi-IPNs exhibited triple- and two-way SMEs under stress-free conditions, indicating that functional SMPs can also be fabricated by designing semi-IPNs composed of homologous polymers.

Experimental section

Materials

All reagents were used as received, unless otherwise specified. Pentaerythritol, acryloyl chloride, tin(II) 2-ethylhexanoate (Sn(Oct)$_2$), CL, and triethylamine were purchased from Tokyo Chemical Industry Co., Ltd, Tokyo, Japan. Xylene, *N*,*N*-dimethylformamide (DMF), tetrahydrofuran (THF), hexane,

acetone, diethyl ether (super dehydrated), methanol, and chloroform-d ($CDCl_3$) with 0.05 v/v% tetramethylsilane (TMS) were purchased from Wako Pure Chemical Industries Ltd, Osaka, Japan. PCL with different molecular weights (average M_n = 10k, 45k and 80k) and benzoyl peroxide (BPO) were purchased from Sigma-Aldrich, MO, USA.

Synthesis of branched PCL macromonomers

PCL diol (2b) and tetra-branched (4b) PCL were synthesised by the ring-opening polymerisation of CL, which was initiated using tetramethylene glycol and pentaerythritol, respectively.[30,31] Thereafter, hydroxyl end groups were modified using acryloyl chloride to introduce a polymerizable acrylate group onto the branch ends. The structure, molecular weight, and introduction rate of the acrylate group for each macromonomer were determined using ^{1}H NMR spectroscopy (400 MHz, JEOL, Tokyo, Japan) and gel permeation chromatography (JASCO International, Tokyo, Japan), respectively (Fig. S1, S2 and Table S1†). The degree of polymerisation of each branch for 2b- and 4bPCL was 18 (2b20PCL) and 10 (4b10PCL), respectively.

Preparation of crosslinked PCL networks and semi-IPNs

The 50 wt% 2b20PCL/50 wt% 4b10PCL macromonomers were dissolved in 45 wt% xylene containing 2-fold molar excess benzoyl peroxide (BPO) at the end-group of macromonomers. The solution was injected between glass slides with a 0.2–1.0 mm thick Teflon spacer. Subsequent thermal polymerisation was conducted at 80 °C for 16 h to obtain the crosslinked 4b10/2b20PCL. As described previously, linear/network blends of PCL, namely PCL semi-IPNs, were prepared in the presence of a given amount (9, 23 and 33 wt% against the total amount of 4b10/2b20 PCL macromonomers) of linear PCL. Specifically, 2b20 PCL and 4b10 PCL macromonomers of equivalent weight ratios in addition to different amounts of linear PCL without polymerisable groups were completely dissolved in 45 wt% xylene with respect to the total macromonomer amount, and then thermally polymerised in the same way as above. The crosslinked 4b10/2b20PCL and PCL semi-IPNs were immersed in acetone to remove the unreacted compounds by swelling and by shrinking them in methanol. These were kept under reduced pressure overnight to obtain completely dry samples. To evaluate the crosslinking efficiency of crosslinked 4b10/2b20PCL and PCL semi-IPNs with different molecular weights, we performed a swelling test. Crosslinked PCL and semi-IPNs were cut into disk shapes approximately 10 mm in diameter (123 ± 14 μm thick) and immersed in DMF for 72 hours until equilibrium swelling was reached. The diameters of three different samples were measured with a digital caliper. The swelling ratio of each sample was simply estimated by its diameter change d/d_0, where d and d_0 are the diameter of the samples in the equilibrium swelling state and the original diameter (before the swelling), respectively. We simultaneously performed gel fraction measurements from the weight of dried samples before and after DMF immersion. The gel fraction was calculated according to the equation $G(\%) = m/m_0 \times 100$, where m is the dry weight after swelling and m_0 is the initial dry weight before swelling. These experiments were conducted for three samples for each composition.

Thermal and crystallinity characterisation

The thermal properties of crosslinked 4b10/2b20PCL, linear PCL with different molecular weights, and PCL semi-IPNs were characterised using differential scanning calorimetry (DSC, 7000X, Hitachi High-Tech Science, Japan). All samples were first equilibrated at 80 °C, and the results of the first cooling process to −20 °C and the second heating process to 80 °C were obtained at a rate of 5 °C min^{-1}. The T_m and enthalpy change of melting were calculated from the peak tops and areas of the endothermic peaks, and the T_c and enthalpy change of crystallisation were calculated from the peak tops and areas of the exothermic peaks of the DSC curves. The degree of crystallinity (χ_c) was calculated using the equation $\chi_c = \Delta H/\Delta H_m$, where ΔH is the enthalpy change of melting for each crosslinked 4b10/2b20PCL, linear PCLs and PCL semi-IPNs, and ΔH_m is the melting enthalpy for 100% crystalline PCL, which is considered to be 136 J g^{-1} according to the literature.[37] Crystallinity changes in the temperature range from 25 to 70 °C were measured using high-temperature X-ray diffraction (HT-XRD, Smart Lab, Rigaku, Japan) using Cu Kα1 radiation with a multitemperature attachment. The crosslinked 4b10/2b20PCL and PCL semi-IPNs containing linear polymers with different molecular weights and a thickness of 1 mm were mounted in a copper sample holder. The area ratios of crystal diffraction peaks shown by PCL were used to trace the relative change in crystallinity as a function of temperature.

Dynamic mechanical and shape memory analyses

The thermomechanical and shape memory properties of crosslinked 4b10/2b20PCL and PCL semi-IPNs were studied using a dynamic mechanical analyser (Discovery DMA 850, TA Instruments, USA). Each film sample was cut into approximately 10 mm (length) × 5 mm (width) × 0.15 mm (thickness) samples and set in the sample clamp of the DMA equipment. To evaluate the thermomechanical properties and thermal transition of the samples, oscillatory tensile deformation was applied with a tensile strain of 2% and a frequency of 1 Hz. The samples were first equilibrated at 80 °C, cooled to −30 °C at a rate of 3 °C min^{-1}, and then heated to 80 °C at the same rate. The changes in the tensile storage modulus (E') for crosslinked 4b10/2b20PCL and PCL semi-IPNs during cooling and heating processes were reported.

Triple- and stress-free two-way SMEs were quantitatively characterised using a Discovery DMA 850 in a controlled stress mode. For the triple-SME, the following two triple-shape creation processes (TSCP-I and TSCP-II) were evaluated:[19] (i) TSCP-I – (1) equilibration at 80 °C (T_{high}) for 5 min, (2) increasing stress to 0.25 MPa at 0.5 MPa min^{-1}, (3) cooling to 25 °C ($T_{mid\text{-}I}$) at 5 °C min^{-1} under a constant stress of 0.5 MPa, (4) reducing stress to 0 MPa at 0.5 MPa min^{-1}, (5) equilibration at 25 °C for 10 min under the above conditions, (6) stress at 0.5 MPa min^{-1} to 1.5 MPa, (7) equilibration at 25 °C for 10 min,

(8) cooling to 0 °C (T_{low}) at 5 °C min^{-1} under a constant stress of 1.5 MPa, (9) reducing stress to 0 MPa at 0.5 MPa min^{-1}, (10) equilibration at 0 MPa for 10 min, (11) heating to 45 °C ($T_{mid\text{-}II}$) at 5 °C min^{-1} under a constant stress of 0 MPa, and (12) heating to 90 °C (>T_{high}) at 5 °C min^{-1} under a constant stress of 0 MPa. The engineered strains obtained in steps (1), (3), (5), (8), (10), (11), and (12) were defined as ε_C, ε_{Bload}, ε_B, ε_{Aload}, ε_A, ε_{Brec}, and ε_{Crec}, respectively. (ii) TSCP-II – (1) equilibration at 80 °C (T_{high}) for 5 min, (2) increasing stress to 0.25 MPa at 0.5 MPa min^{-1}, (3) cooling to 0 °C (T_{low}) at 5 °C min^{-1} under a constant stress of 0.25 MPa, (4) reducing stress to 0 MPa at 0.5 MPa min^{-1}, (5) equilibration at 0 °C for 10 minutes under the above conditions, (6) heating to 45 °C (T_{mid}) at 5 °C min^{-1} under a constant stress of 0 MPa, (7) increasing stress to 1.5 MPa at 0.5 MPa min^{-1}, (8) equilibration at 45 °C for 10 min under the above conditions, (9) cooling to 0 °C (T_{low}) at 5 °C min^{-1} under a constant stress of 1.5 MPa, (10) reducing stress to 0 MPa at 0.5 MPa min^{-1}, (11) equilibration at 0 °C for 10 min under the above conditions, (12) heating to 45 °C (T_{mid}) at 5 °C min^{-1} under a constant stress of 0 MPa, and (13) heating to 90 °C (>T_{high}) at 5 °C min^{-1} under a constant stress of 0 MPa. For TSCP-II, the engineered strains obtained in steps (1), (3), (6), (9), (11), (12), and (13) were defined as ε_C, ε_{Bload}, ε_B, ε_{Aload}, ε_A, ε_{Brec}, and ε_{Crec}, respectively. The shape fixity rate (R_f) and the shape recovery rate (R_r) were calculated using the following equations:

$$R_{fC\to B} = (\varepsilon_B - \varepsilon_C)/(\varepsilon_{Bload} - \varepsilon_C) \times 100 \quad (1)$$

$$R_{fB\to A} = (\varepsilon_A - \varepsilon_B)/(\varepsilon_{Aload} - \varepsilon_B) \times 100 \quad (2)$$

$$R_{rA\to B} = (\varepsilon_A - \varepsilon_{Brec})/(\varepsilon_A - \varepsilon_B) \times 100 \quad (3)$$

$$R_{rB\to C} = (\varepsilon_B - \varepsilon_{Crec})/(\varepsilon_B - \varepsilon_C) \times 100 \quad (4)$$

The Discovery DMA 850 was also used to quantitatively evaluate the stress-free two-way SME in the following controlled stress modes: (1) equilibration at 80 °C (T_{high}) for 5 min, (2) increasing stress to 0.23, 0.40, and 0.53 MPa at 0.5 MPa min^{-1} to achieve different applied strains, (3) cooling to 0 °C (T_{low}) at 5 °C min^{-1} under constant stress, (4) reducing stress to 0 MPa at 0.5 MPa min^{-1}, (5) equilibration at 0 °C for 10 min under these conditions, (6) heating to 42 °C (T_{mid}) at 3 °C min^{-1} under stress-free conditions of 0 MPa, (7) cooling to 0 °C (T_{low}) at 3 °C min^{-1} under stress-free conditions, (8–11) repetition of steps (6) and (7) twice, and (12) heating to 80 °C (T_{high}) at 5 °C min^{-1} under stress-free conditions. The reversible strain (ε_{rev}) was calculated based on the following equation:[29]

$$\varepsilon_{rev} = (\varepsilon_E - \varepsilon_D) \times 100 \quad (5)$$

where ε_E is the deformation achieved at the end of stress-free crystallisation by cooling (T_{low}, steps (7), (9), and (11)), and ε_D is the deformation achieved at the end of melting by heating (T_{mid}, steps (6), (8), and (10)) (see Fig. 6).

Results and discussion

Preparation and thermal analysis of crosslinked PCL networks and semi-IPNs

We have reported that the thermal properties, including T_m, can be precisely controlled by blended crosslinking of PCLs with controlled branching structures and chain lengths.[30–33,35] In particular, crosslinked 4b10PCL/2b20PCL blends obtained using thermal polymerisation with BPO by blending equal amounts of 4b10PCL and 2b20PCL macromonomers exhibited relatively sharp endothermic peaks associated with melting and exothermic peaks associated with crystallisation, with T_m and T_c values of 33.6 and 0.6 °C, respectively (Fig. 1b). Generally, when two PCL macromonomers with different T_m are blended to produce a crosslinked material (*e.g.*, 4b10PCL/4b100PCL blends), the respective polymer chains in the blend are incorporated into a ratio-averaged network structure, such that the T_m of each chain can be fused, resulting in a monophasic crosslinked network that exhibits a single T_m and T_c.[35] Therefore, we hypothesised that by designing PCLs using a semi-IPN structure blended with linear PCLs that are not involved in the crosslinking reaction, it would be possible to fabricate a multiphase network with two distinct peaks (T_m and T_c) derived from the crosslinked PCL network and linear PCLs. Fig. 1c shows the results of DSC measurements of linear PCLs of three different molecular weights (10k, 45k, and 80k) used herein. The T_m values of linear PCLs were 52.7, 56.3, and 57.5 °C corresponding to the molecular weights of 10k, 45k, and 80k, respectively, which shifted to the higher temperature region with increasing molecular weight. In contrast, the enthalpies of melting calculated from the area of the DSC melting curve were 71.1, 69.7, and 43.0 J g^{-1}, which decreased with increasing molecular weight, confirming that molecular weight influences crystallinity.[38] Similarly, the T_c's were 27.4, 28.3. and 26.7 °C for linear PCLs with molecular weights of 10k, 45k and 80k, respectively, with the crystallisation enthalpies decreasing for higher molecular weights.

The results of the swelling test and the gel fraction experiment before and after immersion in a good solvent for crosslinked 4b10PCL/2b20PCL with or without linear PCLs confirmed that the molecular weight and content of linear PCLs did not significantly affect the degree of swelling (d/d_0) and the gel fraction (G) of PCL semi-IPNs (Fig. S3†), suggesting that they have a similar crosslinked structure but linear PCLs are stably entangled in the crosslinked PCL network. Because the T_m of the crosslinked 4b10PCL/2b20PCL and linear PCLs exist 19.1 to 23.9 °C apart, there may be two T_m's or broad melting materials if they are allowed to form independent crystalline phases with each other. Thus, PCL semi-IPNs were prepared by blending and crosslinking 4b10PCL and 2b20PCL macromonomers with linear PCLs, and the effects of the molecular weight of linear PCLs and the blend composition on thermal properties were investigated (Fig. 2). The semi-IPNs composed of linear PCLs with a molecular weight of 10k exhibited a unimodal peak with nearly constant T_m's (36.2 ± 0.1 °C) between 9 and 33 wt% of their content, and a broader tran-

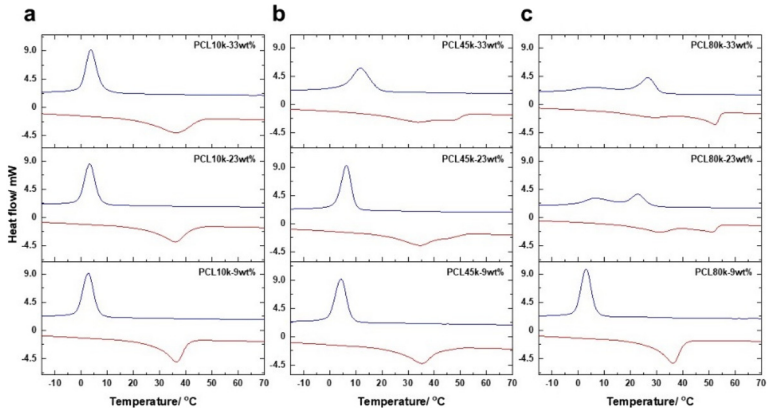

Fig. 2 Representative heating and cooling DSC curves of PCL semi-IPNs with (a) 10k, (b) 45k, and (c) 80k of linear PCL whose content increases from the bottom to top with 9 wt%, 23 wt%, and 33 wt%.

sition at 33 wt% (Fig. 2a and S4†). Similarly, semi-IPNs composed of linear PCLs with a molecular weight of 45k exhibited a unimodal peak indicating the T_m of 34.9 ± 0.5 °C at 9 and 23 wt% content, whereas those at 33 wt% exhibited two distinct melting peaks at 34.1 and 46.1 °C (Fig. 2b and S4†). In the case of the semi-IPN with a molecular weight of 80k of linear PCL, a unimodal T_m of 36.1 °C was observed at 9 wt%, whereas two distinct T_m's were observed at 31.2 and 51.1 °C at 22 wt%, and at 29.4 and 52.1 °C at 33 wt% (Fig. 2c and S4†). For semi-IPNs containing 23 to 33 wt% 80k linear PCL, two distinct exothermic peaks were observed upon crystallisation. These results indicate that the melting behaviour of semi-IPNs is strongly affected by the molecular weight and content of linear PCL in the blend, whereas lower molecular weight materials lead to broadening of the melting peak as the molecular weight increases. In addition to the broadening, a peak on the high-temperature side originating from linear PCL appears, resulting in a two-phase melting, indicating that higher molecular weight is more favourable for crystallisation of linear PCL entangled in the polymer network. The two T_m's are considered to originate from a network consisting of 4b10/2b20 PCL on the low-temperature side and linear PCL on the high-temperature side, which are shifted to the low-temperature side when each exists independently. Hence, in PCL semi-IPNs, the crosslinked network and the linear PCLs entangled in the network form a crystalline phase independently; however, their mutual presence inhibits crystallisation, and their reduced crystallinity may shift T_m toward the lower temperature side.

Temperature-dependent change in crystallinity, and thermomechanical analysis of crosslinked PCL networks and semi-IPNs

Because DSC indicated that PCL semi-IPNs exhibit different thermal properties depending on the molecular weight and linear polymer content, temperature-variable XRD measurements were performed to investigate the temperature-dependent changes in the crystal structure or crystallinity (Fig. 3). The crosslinked 4b10PCL/2b20PCL and PCL semi-IPNs with 33 wt% linear PCL content with molecular weights of 10k, 45k, and 80k exhibited two distinct diffraction peaks at 2θ = 21.4° and 2θ = 23.8°, which correspond to the (110) and (200) planes of PCL's orthorhombic structure.[30,39] The intensity of the diffraction peak characteristic of this PCL decreases with increasing temperature because the crystalline phase melts and shifts to a broad peak indicative of an amorphous phase. In the crosslinked 4b10PCL/2b20PCL, the peak intensity drastically decreases from 38 to 42 °C, thereby transforming to a completely amorphous phase (Fig. 3a). The sharp crystal–amorphous transition exhibited by the crosslinked 4b10PCL/2b20PCL network is affected by the presence of linear PCL chains. For the PCL semi-IPN composed of linear PCL with a molecular weight of 10k, a decrease in diffraction peaks was observed over a wider temperature range (35–48 °C), indicating a continuous and slow crystal–amorphous transition (Fig. 3b). In contrast, PCL semi-IPNs, consisting of 45k and 80k linear PCLs, exhibited a two-phase crystallinity change, with regions of a relatively stable crystalline phase in the ranges 44–48 °C and 40–60 °C (Fig. 3c–e). The XRD measurements were performed on thicker samples, and the mode of temperature modulation was different from that of the DSC measurements, resulting in higher transition temperatures estimated from the XRD measurements compared to the DSC results. However, the XRD measurements revealed the broadening of transition temperature or the appearance of an additional transition temperature derived from linear PCL in the semi-IPNs depending on its molecular weight, which is in perfect agreement with the DSC results.

Thermomechanical analysis was performed to investigate the effect of the molecular weight and content of the linear polymer constituting the PCL semi-IPN on the temperature-dependent mechanical properties. The results obtained by the thermomechanical analysis are important for configuring the experimental conditions for the quantitative analysis of shape memory properties. The tensile storage modulus (E') of crosslinked 4b10/2b20PCL was ~200 MPa near −20 °C. The value of E' decreased slowly with increasing temperature, and then sharply decreased to ~2 MPa at 40 °C near T_m (dotted curves in Fig. 4a, c, and e). When the amorphous sample was heated

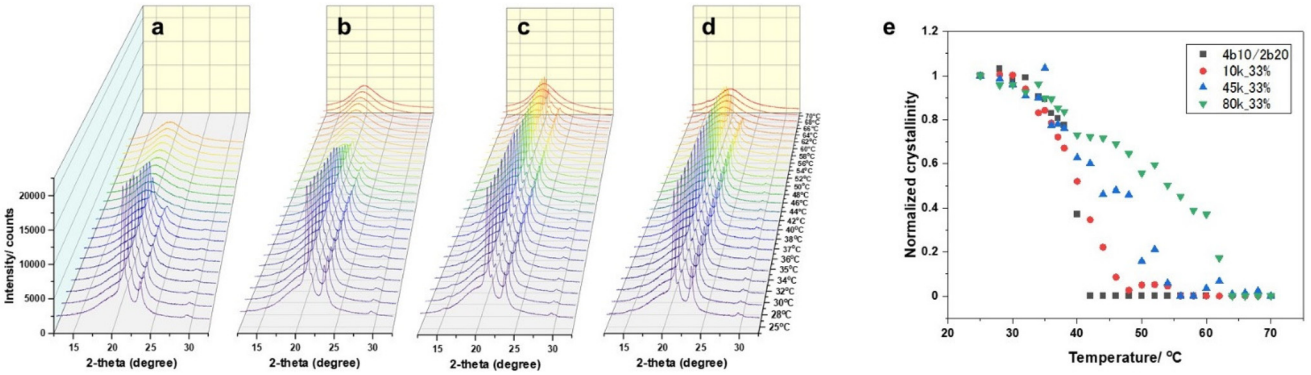

Fig. 3 Temperature-dependent XRD profiles of (a) crosslinked 4b10/2b20PCL and PCL semi-IPNs consisting of 33 wt% linear PCLs with molecular weights of (b) 10k, (c) 45k, and (d) 80k. (e) Relative change in crystallinity with the temperatures of (black) crosslinked PCL and PCL semi-IPNs with (red) 10k, (blue) 45k, and (green) 80k of linear PCL.

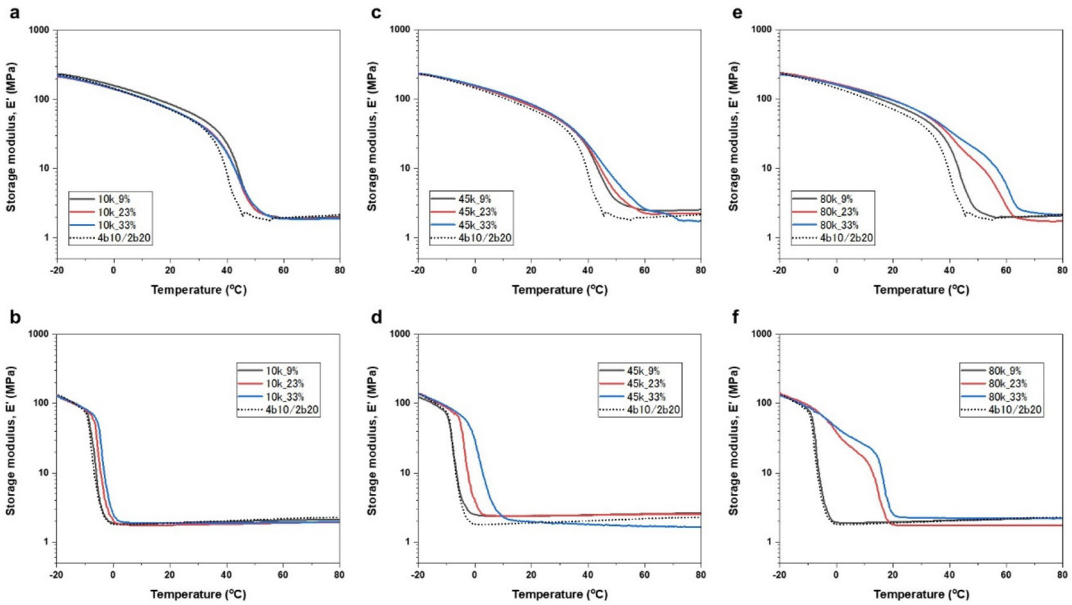

Fig. 4 Temperature-dependent tensile storage modulus (E') for PCL semi-IPNs consisting of (black) 9, (red) 23, (blue) 33 wt% linear PCLs with molecular weights of (a and b) 10k, (c and d) 45k, and (e and f) 80k. The top (a, c, and e) and bottom (b, d, and f) show the behaviour in the heating and cooling processes, respectively. The dotted lines show the results of crosslinked 4b10/2b20PCL.

to 80 °C and subsequently cooled, an increase in E' associated with crystallisation was observed. The temperature at which crystallisation occurred was approximately −2.3 °C, and cooling to −20 °C returned the modulus to nearly its original value (dotted curves in Fig. 4b, d, and f). The PCL semi-IPN with the linear polymer having a molecular weight of 10k exhibited softening on increasing the temperature, similar to that of the crosslinked network without it; however, the transition was more gradual, and T_m shifted to the higher temperature side by approximately 4 °C for all compositions (Fig. 4a). In contrast, the temperature at which crystallisation began was −2.3, −0.2, and 1.3 °C at linear polymer contents of 9, 23, and 33 wt%, respectively, and T_c and T_m shifted toward the higher temperature side with increasing content (Fig. 4b). The PCL semi-IPN composed of the linear polymer with a molecular weight of 45k produced a composition-dependent shift of T_m and T_c toward higher temperature, indicating the broadening of the region where the decrease in E' near the T_m and the increase in E' with crystallisation occur with a gradual transition (Fig. 4c and d). Interestingly, for linear PCL with a molecular weight of 80k, melting and crystallisation were observed as a monophasic transition for the 9 wt% PCL semi-IPN, whereas those with 23 and 33 wt% content exhibited two distinct melting (41.5 °C and 56.6 °C at 23 wt%, 39.2 °C and 60.8 °C at 33 wt%) and crystallisation processes (9.6 °C and 18.5 °C at 23 wt%, and 11.3 °C and 20.3 °C at 33 wt%) (Fig. 4e and f). This was consistent with the results of DSC and XRD measurements, indicating that PCL semi-IPNs consisting of

80k linear PCL with a higher content exhibit two T_m and T_c values, which cause independent melting and crystallisation of the crosslinked PCL network and linear PCL, respectively. Hence, semi-IPNs composed of homologous polymers facilitate the design of multiphase polymer networks.

Quantitative analysis of the triple-SME in multiphase PCL semi-IPNs

As mentioned previously, the PCL semi-IPN containing 23 wt% linear PCL with a molecular weight of 80k was observed to be a multiphase polymer network with two distinct T_m and T_c. The characteristics of the PCL semi-IPN were utilised to verify its feasibility as a triple-SMP. Two triple-shape creation processes (TSCP) proposed by Lendlein *et al.* were examined.[19] TSCP-I is a process consisting of the following sequence: T_{high} → deformation (applied stress) → $T_{mid\text{-}I}$ → deformation (applied stress) → T_{low} → $T_{mid\text{-}II}$ → T_{high}, and TSCP-II is a process consisting of the following sequence: T_{high} → deformation (applied stress) → T_{low} → T_{mid} → deformation (applied stress) → T_{low} → T_{mid} → T_{high}. TSCP-I and TSCP-II have different cooling and deformation processes.

Fig. 5a shows a typical stress–strain–temperature diagram for the shape program and recovery of the PCL semi-IPN containing 23 wt% linear PCL with a molecular weight of 80k according to TSCP-I. Herein, based on the results of thermo-mechanical analysis, T_{high}, $T_{mid\text{-}I}$, $T_{mid\text{-}II}$, and T_{low} were set to 80, 25, 45, and 0 °C, respectively (Fig. 4). Under T_{high} conditions, a stress of 0.25 MPa was applied to deform the sample from the original state of shape C, and the temperature was reduced to $T_{mid\text{-}I}$. This cooling process caused a further increase in strain (ε_{Bload} = 38.2%) by CIE from the initial applied strain (ε_B^0 = 27.9%) despite the cooling process being carried out under constant stress. After the temperature reached $T_{mid\text{-}I}$, the stress-relieved state was shape B (ε_B = 26.6%). Hence, even at $T_{mid\text{-}I}$ (25 °C), the sample was able to crystallise and fix the applied strain, although not completely (see below for details). Thereafter, while keeping $T_{mid\text{-}I}$ constant, a stress of 1.5 MPa was applied to further deform the sample, followed by decreasing the temperature to T_{low} under constant stress. This cooling process also caused CIE, with an ε_{Aload} of 70.5% and shape A with an ε_A of 67.0% after stress removal. Increasing temperature under stress-free conditions decreased the fixed strain, *i.e.*, shape recovery from shape A to a recovered shape B (ε_{Brec} = 30.4%) at 45 °C ($T_{mid\text{-}II}$), and to a recovered permanent shape C at 80 °C (T_{high}) (ε_{Crec} = 1.97%).

Subsequently, the triple-SME of the same PCL semi-IPN was examined according to TSCP-II (Fig. 5b) wherein T_{high}, T_{mid}, and T_{low} were set to 80, 45, and 0 °C, respectively. Similar to TSCP-I, a stress of 0.25 MPa was applied to deform the sample at T_{high}, and the temperature was reduced to T_{low}. During the cooling process, an increase in strain with CIE was observed near 20 °C, and ε_{Bload} was 54.5% when the temperature reached 0 °C (T_{low}). Compared to TSCP-I, the larger ε_{Bload} is attributed to more accelerated crystallisation and larger CIE because of cooling down to T_{low}. The strain after removing the stress at T_{low} was 54.1%. A slight strain recovery or shrinkage occurred as the temperature was increased, and the state maintained at 45 °C was shape B (ε_B = 43.7%). As the temperature increased to T_{mid}, a stress of 1.5 MPa was applied to further deform the sample, and the temperature was again decreased to T_{low} under constant stress. This cooling process caused a relatively large CIE, resulting in an ε_{Aload} of 166%, and shape A with an ε_A of 160% was obtained after the stress was fully removed. For shape A, increasing the temperature to T_{mid}

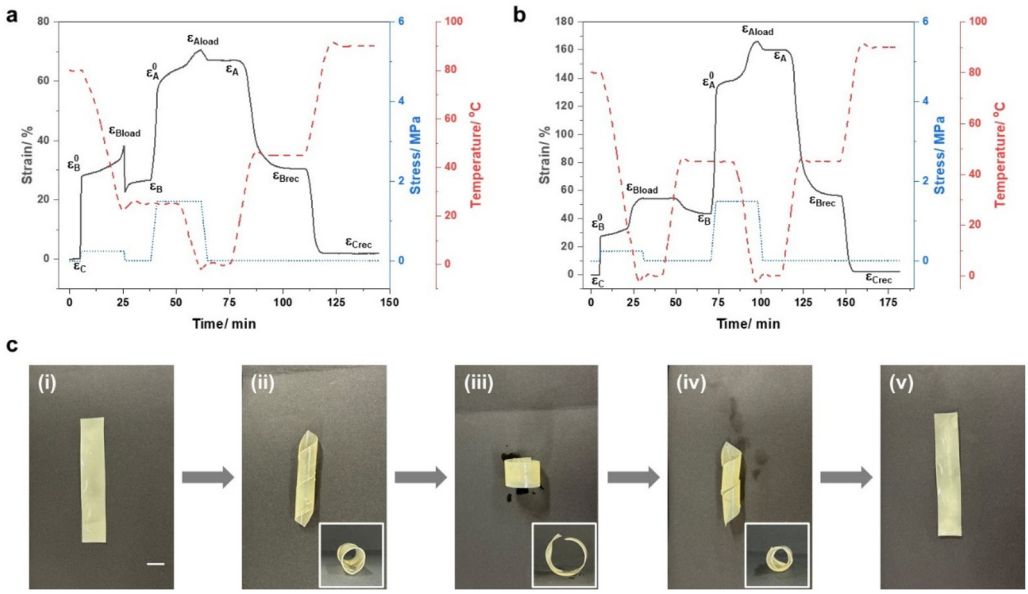

Fig. 5 Triple-SME of PCL semi-IPNs consisting of 23 wt% linear PCL with a molecular weight of 80k. Quantitative thermal mechanical cycle test for (a) TSCP-I and (b) TSCP-II. (c) Visual demonstration of the triple-SME for the PCL semi-IPN.

resulted in a recovered shape B (ε_{Brec} = 56.2%) and eventually, the shape recovered to a permanent shape C (ε_{Crec} = 2.26%) at T_{high}. The fact that cross-linked 4b10/2b20PCLs without linear PCLs did not show the triple-SME in either TSCP-I or TSCP-II also strongly suggests the importance of multiphase formation by the semi-IPN structure (Fig. S5†).

The results of shape fixity (R_f) and recovery (R_r) ratios for the three different shapes in TSCP-I and TSCP-II are shown in Table 1. The shape fixity ratio ($R_{fC\to B}$) from shape C to B under the same loading stress conditions was 69.6% for TSCP-I, whereas it was as high as 80.2% for TSCP-II. This is because in TSCP-I, the temperature at which shape B was fixed was 25 °C ($T_{mid\text{-}I}$) whereas in TSCP-II, the crystallisation required to fix the shape was more accelerated because cooling to 0 °C (T_{low}) occurred. Therefore, the $R_{fC\to B}$ of TSCP-I may be improved by setting $T_{mid\text{-}I}$ to a lower temperature or increasing the time at $T_{mid\text{-}I}$. Parameters other than $R_{fC\to B}$, such as the shape fixity ratio from shape B to A ($R_{fB\to A}$) and the shape recovery ratio from shape A to B ($R_{rA\to B}$) and shape B to C ($R_{rB\to C}$), were approximately equal to or greater than 90%, indicating that the PCL semi-IPN has high capability for the triple-SME. A similar triple-SME was observed for at least three cycles despite both TSCP-I and TSCP-II, indicating that the PCL semi-IPN has excellent repeatability under the same conditions (Fig. S6†).

To demonstrate the triple-SME, macroscopic changes in shape fixation and recovery were examined using the aforementioned TSCP-II (Fig. 5c). First, a flat rectangular sample (i) was deformed into a spiral shape at 80 °C (T_{high}), cooled to 4 °C (T_{low}), and heated to 40 °C (T_{mid}) to obtain a temporary spiral shape (ii). Thereafter, the sample was deformed into a ring shape and cooled again to T_{low} at which the ring shape was fixed as the second temporary shape (iii). Raising the temperature of the ring-shaped sample from T_{mid} to T_{high} caused it to undergo a spiral shape once (iv) and return to its original flat and permanent shape (v). In summary, the semi-IPN structure consisting of a 4b10/2b20 PCL network, which originally exhibited a monophasic transition, and linear PCL with a molecular weight of 80k, introduced an additional phase transition based on the linear PCL. Furthermore, the obtained multiphase PCL semi-IPN facilitated the development of an excellent triple-SME.

Table 1 Triple-shape memory properties of PCL semi-IPNs characterized by a thermomechanical cycle test

SM performance	TSCP-I	TSCP-II
$R_{fC\to B}$	69.6%	80.2%
$R_{fB\to A}$	95.0%	96.4%
$R_{rA\to B}$	90.6%	89.3%
$R_{rB\to C}$	92.6%	94.8%

Stress-free two-way SME in multiphase PCL semi-IPNs

In addition to the triple-SME, designing multiphase networks to achieve a stress-free two-way (reversible) SME is crucial.[23] Thus, the two-way SME of the PCL semi-IPN that contains 23 wt% linear PCL with a molecular weight of 80k having two values of T_m and T_c, was evaluated using the following thermomechanical protocol (Fig. 6a). Initially, a stress of 0.4 MPa was

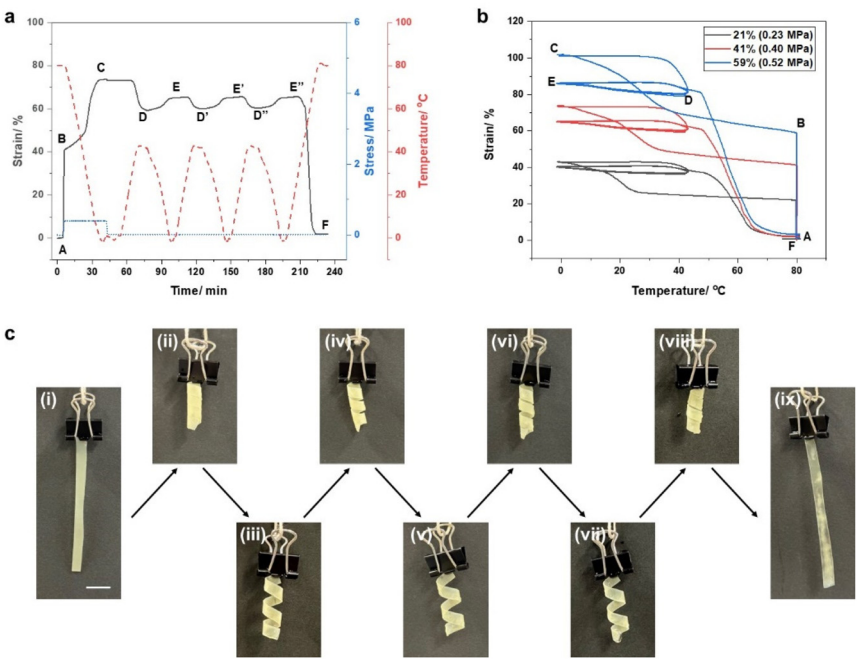

Fig. 6 (a) Stress-free two-way SME of PCL semi-IPNs consisting of 23 wt% linear PCL with a molecular weight of 80k evaluated over three cycles. (b) Strain *versus* temperature curves for the stress-free two-way SME under various applied strains. (c) Visual demonstration of the stress-free two-way SME for the PCL semi-IPN.

applied at 80 °C to deform the sample up to 41% strain, and the temperature was lowered to 0 °C under constant stress conditions. Thereafter, the temperature was raised to 42 °C under stress removal, equilibrated, and lowered to 0 °C. After this process was repeated thrice, the temperature was raised to 80 °C to reset the temporarily strain-fixed sample shape. Although CIE was observed during the initial cooling process, the deformed shape was nearly maintained upon unloading, *i.e.*, with a shape-fixation ratio of >99%. Heating after unloading decreased the strain, whereas the subsequent cooling of the sample increased the strain. The variation in strain during these processes was nearly identical for at least three cycles, which can be attributed to the MIC and CIE exhibited by the 4b10/2b20PCL network forming the crystalline phase at a lower temperature. This strain variation is influenced by stress loading and generally, the deformation increases with increasing the loaded strain.[24,29] Therefore, the stress applied to the PCL semi-IPN containing 23 wt% of 80k linear PCL at 80 °C was controlled in the aforementioned thermomechanical protocol, and the stress-free two-way SME was examined at applied strains of 21% (0.23 MPa), 41% (0.40 MPa), and 59% (0.52 MPa) (Fig. 6b). For all these conditions, the strain variations during the post-unloading temperature variations exhibited similar deformation behaviour for at least three cycles. The reversible strain ($\varepsilon_{rev} = (\varepsilon_E - \varepsilon_D)$) at 21, 41, and 59% was 4.2, 5.6, and 7.1%, respectively, thereby confirming the monotonic increase with increasing initial stress load.

To demonstrate the stress-free two-way SME, the macroscopic deformation behaviour was studied (Fig. 6c). Initially, a rectangular sample (i) was deformed into a spiral shape at 80 °C and cooled to 4 °C to fix it as a temporary shape (ii). Thereafter, the pitch of the spiral increased and changed to an open spiral shape (iii) after heating to 40 °C. When cooled to 4 °C, the pitch of the spiral decreased and returned to a closed spiral shape (iv). The opening and closing of the spiral shape upon heating and cooling was almost reversible for at least three cycles (ii–viii). Upon heating to 80 °C, the temporary shape disappeared, and the original rectangular, permanent shape was restored (ix). In this system, the length variation in the long axis direction of the spiral was ~15%, confirming the reversible shape change under stress-free conditions macroscopically.

Conclusions

The findings of this study indicate that a multiphase polymer network exhibiting two distinct transition temperatures (T_m and T_c) can be designed, even in semi-IPNs comprising the homologous polymer PCL. To achieve this, it is crucial to control the crystallinity of the crosslinked network and linear polymers entangled in it. Usually, PCL has a melting temperature of 60 °C; however, the crystallinity of 4b10/2b20PCL decreases significantly after crosslinking, resulting in the formation of a network that exhibits monophasic T_m near the biological temperature. Linear PCLs constituting semi-IPNs are crucial for higher molecular weight PCLs and higher amounts of PCLs, thereby favouring crystallisation in the interpenetrated network. Thus, fabricating PCL semi-IPNs with two independent crystalline phases is possible, and the resulting material exhibits a triple-SME and stress-free two-way SME. Compared to previously reported multiphase polymer networks exhibiting two transition temperatures, the proposed PCL semi-IPNs may require more severe temperature settings for TSCP and may be less operable because the transition temperatures are not well separated. Consequently, the triple-SME can be observed upon smaller temperature changes. Currently, the maximum stress-free two-way SME of PCL semi-IPNs exhibits a maximum reversible strain of 7.1%; however, the magnitude of this deformation may be controlled using the magnitude of the applied strain and the temperature of operation. Additionally, more detailed design of network formation and PCL structures entangled in the network will pave the way for designing materials that exhibit even greater deformation. The T_m of the crystalline phase driven on the low-temperature side of PCL semi-IPNs operates near the biological temperature of 40 °C. Therefore, PCL semi-IPNs may find applications in the fields of actuators, robotics, and biomedical devices with smart functions.

Author contributions

Koichiro Uto: conceptualisation, methodology, formal analysis, funding acquisition, and writing – original draft; Yoshitaka Matsushita: methodology and analysis; Mitsuhiro Ebara: supervision and writing – review & editing.

Conflicts of interest

There are no conflicts to declare.

Acknowledgements

The authors sincerely thank Mr Yuichi Sasaki, Ms Rie Yamamoto, Ms Chinami Azechi, and Ms Minori Kouno for supporting the experiments. This study was supported by a JSPS KAKENHI Grant-in-Aid for Scientific Research (C) (JP21K12696), a Grant-in-Aid for Scientific Research (B) (JP19H04476) a Grant-in-Aid for Transformative Research Areas (A) (JP20H05877), and the Innovative Science and Technology Initiative for Security Grant Number JPJ004596, ATLA, Japan.

References

1 A. Lendlein, A. M. Schmidt and R. Langer, *Proc. Natl. Acad. Sci. U. S. A.*, 2001, **98**, 842–847.
2 A. Lendlein and R. Langer, *Science*, 2002, **296**, 1673–1676.

3 A. Lendlein, H. Jiang, O. Junger and R. Langer, *Nature*, 2005, **434**, 879–882.
4 H. Koerner, G. Price, N. A. Pearce, M. Alexander and R. A. Vaia, *Nat. Mater.*, 2004, **3**, 115–120.
5 R. Mohr, K. Kratz, T. Weigel, M. Lucka-Gabor, M. Moneke and A. Lendlein, *Proc. Natl. Acad. Sci. U. S. A.*, 2006, **103**, 3540–3545.
6 C. Lin, J. Lv, Y. Li, F. Zhang, J. Li, Y. Liu, L. Liu and J. Leng, *Adv. Funct. Mater.*, 2019, **29**, 1906569.
7 J. Delaey, P. Dubruel and S. Van Vlierberghe, *Adv. Funct. Mater.*, 2020, **30**, 1909047.
8 Y. Liu, H. Du, L. Liu and J. Leng, *Smart Mater. Struct.*, 2014, **23**, 023001.
9 T. Chen, O. R. Bilal, R. Lang, C. Daraio and K. Shea, *Phys. Rev. Appl.*, 2019, **11**, 064069.
10 T. Suman, in *Textiles for Advanced Applications*, ed. K. Bipin and T. Suman, IntechOpen, Rijeka, 2017, ch. 12, DOI: **10.5772/intechopen.69742**.
11 D. J. Roach, C. Yuan, X. Kuang, V. C.-F. Li, P. Blake, M. L. Romero, I. Hammel, K. Yu and H. J. Qi, *ACS Appl. Mater. Interfaces*, 2019, **11**, 19514–19521.
12 A. Lendlein, *Sci. Robot*, 2018, **3**, eaat9090.
13 Y.-F. Zhang, N. Zhang, H. Hingorani, N. Ding, D. Wang, C. Yuan, B. Zhang, G. Gu and Q. Ge, *Adv. Funct. Mater.*, 2019, **29**, 1806698.
14 T. Sekitani, U. Zschieschang, H. Klauk and T. Someya, *Nat. Mater.*, 2010, **9**, 1015–1022.
15 H. Gao, J. Li, F. Zhang, Y. Liu and J. Leng, *Mater. Horiz.*, 2019, **6**, 931–944.
16 A. Lendlein and S. Kelch, *Angew. Chem., Int. Ed.*, 2002, **41**, 2034–2057.
17 C. Liu, H. Qin and P. T. Mather, *J. Mater. Chem.*, 2007, **17**, 1543–1558.
18 I. Bellin, S. Kelch, R. Langer and A. Lendlein, *Proc. Natl. Acad. Sci. U. S. A.*, 2006, **103**, 18043–18047.
19 M. Behl and A. Lendlein, *J. Mater. Chem.*, 2010, **20**, 3335–3345.
20 T. Xie, *Nature*, 2010, **464**, 267–270.
21 Y. Shao, C. Lavigueur and X. X. Zhu, *Macromolecules*, 2012, **45**, 1924–1930.
22 M. Behl, I. Bellin, S. Kelch, W. Wagermaier and A. Lendlein, *Adv. Funct. Mater.*, 2009, **19**, 102–108.
23 A. Lendlein and O. E. C. Gould, *Nat. Rev. Mater.*, 2019, **4**, 116–133.
24 T. Chung, A. Romo-Uribe and P. T. Mather, *Macromolecules*, 2008, **41**, 184–192.
25 S. J. Hong, W.-R. Yu and J. H. Youk, *Smart Mater. Struct.*, 2010, **19**, 035022.
26 M. Behl, K. Kratz, J. Zotzmann, U. Nöchel and A. Lendlein, *Adv. Mater.*, 2013, **25**, 4466–4469.
27 T. Xiang, J. Wang, L. Jia, P. Wang and S. Zhou, *Polym. Chem.*, 2022, **13**, 6614–6624.
28 L. Xiao, M. Wei, M. Zhan, J. Zhang, H. Xie, X. Deng, K. Yang and Y. Wang, *Polym. Chem.*, 2014, **5**, 2231–2241.
29 N. Inverardi, M. Toselli, G. Scalet, M. Messori, F. Auricchio and S. Pandini, *Macromolecules*, 2022, **55**, 8533–8547.
30 K. Uto, K. Yamamoto, S. Hirase and T. Aoyagi, *J. Controlled Release*, 2006, **110**, 408–413.
31 M. Ebara, K. Uto, N. Idota, J. M. Hoffman and T. Aoyagi, *Adv. Mater.*, 2012, **24**, 273–278.
32 K. Uto, T. Aoyagi, C. A. DeForest, A. S. Hoffman and M. Ebara, *Adv. Healthcare Mater.*, 2017, **6**, 1601439.
33 K. Uto, T. Aoyagi, C. A. DeForest and M. Ebara, *Biomater. Sci.*, 2018, **6**, 1002–1006.
34 A. Lendlein, A. M. Schmidt, M. Schroeter and R. Langer, *J. Polym. Sci., Part A: Polym. Chem.*, 2005, **43**, 1369–1381.
35 A. Fulati, K. Uto and M. Ebara, *Polymer*, 2022, **14**, 4740.
36 E. D. Rodriguez, X. Luo and P. T. Mather, *ACS Appl. Mater. Interfaces*, 2011, **3**, 152–161.
37 B. Lepoittevin, M. Devalckenaere, N. Pantoustier, M. Alexandre, D. Kubies, C. Calberg, R. Jérôme and P. Dubois, *Polymer*, 2002, **43**, 4017–4023.
38 W.-C. Ou-Yang, L.-J. Li, H.-L. Chen and J. C. Hwang, *Polym. J.*, 1997, **29**, 889–893.
39 A. Babaie, M. Rezaei and R. L. M. Sofla, *J. Mech. Behav. Biomed. Mater.*, 2019, **96**, 53–68.